2016 IEEE/RSJ International Conference on Intelligent Robots and Systems (IROS)
Daejeon Convention Center
October 9-14, 2016, Daejeon, Korea

A Robust Adaptive Control of Mecanum Wheel Mobile Robot: Simulation and Experimental Validation

Veer Alakshendra, Shital S. Chiddarwar

Abstract— **Omnidirectional mobile robots with four Mecanum wheels are used in various homes, military, nuclear power plant, industrial, hospital and space applications. A lot of research has been done using three universal wheels but trajectory control for four Mecanum wheeled mobile robot (FMWMR) in presence of uncertainties still needs attention. Thus, to obtain smooth motion of mobile robots, with chattering free control input, in presence of uncertainties and external force disturbances, a robust and adaptive control is necessary. In view of these aspects, this paper extends the use of adaptive sliding mode controller for trajectory tracking of FMWMR. The effectiveness of proposed controller is verified using two case problems. Simulation results are presented for the verification of proposed controller for FMWMR. Further, experiments are conducted using position and orientation sensor to show the performance of the controller in real world environment. Simulation and experimental results revealed that FMWMR is capable of tracking any type of trajectories.**

I. INTRODUCTION

In recent years, the study of mobile robots subjected to non linear disturbances has gained popularity. Mobile robots are classified as conventional wheeled mobile robots and omnidirectional wheel mobile robots. Owing to advantages such as better maneuverability, ability to turn in any direction without reorientation, and capability to move in confined spaces, omnidirectional wheeled mobile robot has become a major interest for research. Among various types of omnidirectional robots, four wheeled omnidirectional mobile robot (FMWMR) is one of them, which is a holonomic system that has three degrees of freedom in a horizontal plane [1].

The kinematic and dynamic modeling of an omnidirectional wheeled mobile robot has been investigated by many researchers. [2] proposed a practical opproach to model an omnidirectional robot. The dynamics of a FMWMR is well presented in [3]. As these mobile robots can be extensively used for transporting and carrying materials in hospitals, nuclear power plants, and industries, it is inevitable to derive the dynamic equation where linear and angular velocities are the output states. In order to do the same, we have used Newton Euler method to derive a generalised equation of motion in world coordinate frame.

*Research supported by Visvesvarya National Institute of Technology, Nagpur-440010, India

Veer Alakshendra is with Department of Mechanical Engineering, Visvesvarya National Institute of Technology, Nagpur-440014, India (phone: +91 8446985971; e-mail:alakshendra.veer@gmail.com)

Shital S. Chiddarwar is with Department of Mechanical Engineering, Visvesvarya National Institute of Technology, Nagpur-440014, India (e-mail:shitalsc@mec.vnit.ac.in)

As the mobile robots are exposed to dynamic environment, non linearities associated with it are bound to alter the desired trajectory. Hence, a non linear controller is necessary to minimize the tracking error. Out of various non linear control methods such as sliding mode control, H_∞ control, artificial intelligence techniques etc., sliding mode control has gained popularity owing to advantages such as insensitivity to disturbances [4] and [5]. Inspired by the past researchers, sliding mode control (SMC) method is selected in this work to control the FMWMR subjected to uncertainties and friction. Although, sliding mode control is robust against uncertainties but its implementation becomes difficult when the bounds of uncertainties keeps changing. Moreover, it has a major disadvantage of increased chattering due to use of switching function during the sliding phase. Hence, to counter these disadvantages adaptive control law has been implemented [6] and [7].

The main goal of our work is to make the FMWMR to track the reference trajectory in presence of uncertainties and external force disturbances. The major contributions, comparison with previous works and organization of this paper are summarized below:

1) In the previous work a generalized dynamic equation in world coordinate frame taking kinematic equations into consideration was not derived which has been done in our paper (Section II). Moreover, we have not simplified the obtained second order nonlinear equation by using linearization methods.

2) The previous researchers have derived adaptive sliding mode control law for either a single input single output (SISO) system such as inverted pendulum or on a conventional mobile robots, whereas in our work we have derived it for a FMWMR (Section III)

3) Further as our mobile robot has three degrees of freedom, we have shown two trajectories in which the angular displacement is kept constant in first trajectory whereas in the second it is changing with time (Section IV).

4) At last, most of the earlier work based on SMC has been reported based on simulation results whereas we have attempted the proposed algorithm on a real robot using position and orientation sensors (Section VI).

Conclusions drawn from this study are presented in Section VI.

II. KINEMATIC AND DYNAMIC MODELING OF FMWMR

A four wheeled omnidirectional mobile robot has four Mecanum wheels in which peripheral rollers are inclined at a

constant slope angle (γ). In this case $\gamma = 45^0$, hence the wheel moves freely at an angle 45^0 with the driven motion.

A. FMWMR kinematics

Fig. 1 shows the schematic of a FMWMR. Let O_q, O_r, and $O_{wi}(i = 1,2,3,4)$ are world frame, mobile robot moving frame and wheel coordinate frame respectively. If $P_{wi} = [x_{wi} \quad y_{wi} \quad \phi_{wi}]$ is the position vector of wheel in O_{wi}, then

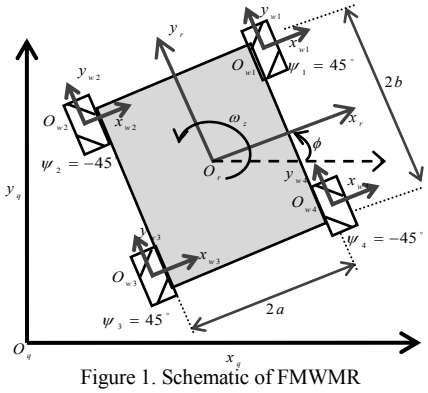

Figure 1. Schematic of FMWMR

velocity vector is given as

$$\dot{P}_{wi} = \begin{bmatrix} \dot{x}_{wi} \\ \dot{y}_{wi} \\ \dot{\phi}_{wi} \end{bmatrix} = \begin{bmatrix} 0 & r_i \sin(\gamma_i) & 0 \\ R_i & -r_i \cos(\gamma_i) & 0 \\ 0 & 0 & 1 \end{bmatrix} \begin{bmatrix} \theta_{ix} \\ \theta_{ir} \\ \theta_{iz} \end{bmatrix} \tag{1}$$

where θ_{ix}, θ_{ir}, and θ_{iz} are wheel angular velocity around the hub, angular velocity of roller and wheel angular velocity about the contact point, R_i is the wheel radius and r_i is the roller radius. Using transformation robot velocity vector in frame O_r is written as

$$\dot{P}_r = \begin{bmatrix} \dot{x}_r \\ \dot{y}_r \\ \dot{\phi}_r \end{bmatrix} = \begin{bmatrix} 1 & 0 & d_{ix} \\ 0 & 1 & d_{iy} \\ 0 & 0 & 1 \end{bmatrix} \begin{bmatrix} \dot{x}_{wi} \\ \dot{y}_{wi} \\ \dot{\phi}_{wi} \end{bmatrix} \tag{2}$$

where d_{ix} and d_{iy} are translational distance between O_r and O_{wi} in x and y direction respectively. Substituting (1) in (2)

$$\dot{P}_r = J_i \dot{q}_i \tag{3}$$

where $J_i \in R^{3\times3}$ is the Jacobian matrix of ith wheel and is obtained as $J_i = \begin{bmatrix} 0 & r_i \sin(\gamma_i) & d_{ix} \\ R_i & -r_i \cos(\gamma_i) & d_{iy} \\ 0 & 0 & 1 \end{bmatrix}$ and $\dot{q}_i = [\theta_{ix} \quad \theta_{ir} \quad \theta_{iz}]$.

Remark 1: $|J_i| = -r_i R_i \sin(\gamma_i) = 0 \ \forall \ \gamma_i = 0$. Hence, there is no singularity present in Mecanum wheels.

Remark 2: Rank(J_i)=3, therefore each wheel has three degrees of freedom (DOF).

Considering all wheels to be identical, kinematic parameters for each wheel can be written as $R_i = R, r_i = r, d_{1x} = a, d_{1y} = b,$

$d_{2x} = -a, d_{2y} = b, d_{3x} = -a, d_{3y} = -b, d_{4x} = a, d_{4y} = -b$. Thus,

$$J_1 = \begin{bmatrix} 0 & r/\sqrt{2} & a \\ R & -r/\sqrt{2} & b \\ 0 & 0 & 1 \end{bmatrix}, \ J_2 = \begin{bmatrix} 0 & -r/\sqrt{2} & a \\ R & -r/\sqrt{2} & -b \\ 0 & 0 & 1 \end{bmatrix},$$

$$J_3 = \begin{bmatrix} 0 & r/\sqrt{2} & -a \\ R & -r/\sqrt{2} & -b \\ 0 & 0 & 1 \end{bmatrix}, \ J_4 = \begin{bmatrix} 0 & -r/\sqrt{2} & -a \\ R & -r/\sqrt{2} & b \\ 0 & 0 & 1 \end{bmatrix}.$$ Using (3) and Jacobian matrices for each wheel, inverse kinematics model of the mobile robot is obtained as [8]

$$\begin{bmatrix} \dot{x}_r \\ \dot{y}_r \\ \dot{\phi}_r \end{bmatrix} = \frac{R}{4} \begin{bmatrix} -1 & 1 & -1 & 1 \\ 1 & 1 & 1 & 1 \\ 1/a+b & -1/a+b & -1/a+b & 1/a+b \end{bmatrix} \begin{bmatrix} \dot{\theta}_1 \\ \dot{\theta}_2 \\ \dot{\theta}_3 \\ \dot{\theta}_4 \end{bmatrix} \tag{4}$$

where $\dot{\theta}_i(i = 1,2,3,4)$ is the angular velocity of each wheel. Further, velocity vector in world coordinate frame O_q is given as $\dot{P}_q = [\dot{x}_q \quad \dot{y}_q \quad \dot{\phi}] = R(\phi)\dot{P}_r$, where $R(\phi) = \begin{bmatrix} \cos(\phi) & -\sin(\phi) & 0 \\ \sin(\phi) & \cos(\phi) & 0 \\ 0 & 0 & 1 \end{bmatrix}$ is the rotation matrix of moving frame O_r with respect to frame O_q.

B. FMWMR dynamics

For the dynamic modeling of the FMWMR it is assumed that coordinate frame O_r lies on the center of gravity of the robot(Fig. 2).

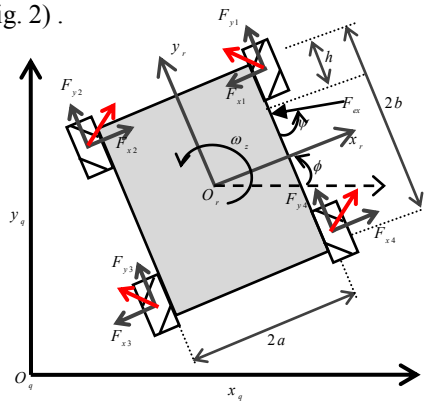

Figure 2. Force diagram of FMWMR

According to Newton's second law, dynamic equation in coordinate frame O_r is written as

$$M\ddot{S}_q = F_q \tag{5}$$

$$\begin{bmatrix} M & 0 \\ 0 & M \end{bmatrix} \begin{bmatrix} \ddot{x}_q \\ \ddot{y}_q \end{bmatrix} = \begin{bmatrix} F_{qx} \\ F_{qy} \end{bmatrix} \tag{6}$$

where M is the mass of the mobile robot, S_q and F_q are the position and force vector respectively in O_q. Let

${}^qR_r(\phi) = \begin{bmatrix} \cos(\phi) & -\sin(\phi) \\ \sin(\phi) & \cos(\phi) \end{bmatrix}$ is the transformation matrix,

such that $\dot{S}_q = {}^qR_r(\phi)\dot{S}_r$ and $F_q = {}^qR_r(\phi)F_r$. Thus (5), can be modified as

$$M\left({}^qR_r(\phi)\ddot{S}_r + {}^qR_r(\dot{\phi})\dot{S}_r\right) = {}^qR_r(\phi)F_r \tag{7}$$

$$\begin{bmatrix} M & 0 \\ 0 & M \end{bmatrix}\begin{bmatrix} \ddot{x}_r - \dot{\phi}\dot{y}_r \\ \ddot{y}_r - \dot{\phi}\dot{x}_r \end{bmatrix} = \begin{bmatrix} F_{xr} \\ F_{yr} \end{bmatrix} - \begin{bmatrix} \beta_x\dot{x}_r \\ \beta_y\dot{y}_r \end{bmatrix} + \begin{bmatrix} -F_{ex}\cos(\psi) \\ F_{ex}\sin(\psi) \end{bmatrix} \tag{8}$$

where $\dot{S}_r$ and F_r are the position and force vector respectively in O_r. F_{xr} and F_{yr} are total forces in x and y direction respectively. β_x and β_y are linear friction coefficients in x and y direction respectively. F_{ex} is the external force disturbance acting at an angle ψ with y_r direction at a distance h from upper edge of the mobile robot. Further Euler equation is written as

$$I_q\ddot{\phi} = \tau - \beta_z\dot{\phi} + F_{ex}\cos(\psi)a - F_{ex}\sin(\psi)(b-h) \tag{9}$$

where I_q is the moment of inertia of the robot about its c.g, τ is the moment about the c.g and β_z is the linear coefficient of friction in z direction. The driving F_{di} is generated by the DC motor attached to each wheel which is given as [9]

$$F_{di}(i = 1,2,3,4) = \alpha u_i - \beta r_i\theta_i \tag{10}$$

where u_i is the input voltage at each motor, α and β are DC motor coefficients obtained from manufacturer's catalogue. Utilizing (10) F_{xr}, F_{yr} and τ can be written as

$$F_{xr} = \frac{1}{2}(-F_{d1} + F_{d2} - F_{d3} + F_{d4}) \tag{11}$$

$$F_{yr} = \frac{1}{2}(F_{d1} + F_{d2} + F_{d3} + F_{d4}) \tag{12}$$

$$\tau = \frac{a}{2}(F_{d1} - F_{d2} - F_{d3} + F_{d4}) + \frac{b}{2}(F_{d1} - F_{d2} - F_{d3} + F_{d4}) \tag{13}$$

Using (8) to (13) the dynamic equations for the FMWMR can be represented in the form

$$\ddot{x}(t) = f(x) + g(x)u(t) + \xi(t,u(t)) \tag{14}$$

where $\ddot{x}(t) = \begin{bmatrix}\ddot{x}_q & \ddot{y}_q & \ddot{\phi}\end{bmatrix}^T$,

$u(t) = \begin{bmatrix}u_1 & u_2 & u_3\end{bmatrix}^T$,

$$f(x) = \begin{bmatrix} (1/2M)(a_1\dot{y}_q + a_2\dot{y}_q + 2\beta_y\dot{x}_q + a_3\dot{x}_q + a_4 + a_5 + 4\beta\dot{x}_q) \\ (1/2M)(b_1\dot{x}_q + b_2\dot{x}_q + 2\beta_x\dot{y}_q + b_3\dot{y}_q + b_4 + b_5 + 4\beta\dot{y}_q) \\ (-1/2I_q)(c_1\dot{\phi} + c_2 + c_3 + c_4) \end{bmatrix}$$

, $g(x) = \begin{bmatrix} \bar{a}_{11} & \bar{a}_{12} & \bar{a}_{13} & \bar{a}_{14} \\ \bar{b}_{11} & \bar{b}_{12} & \bar{b}_{13} & \bar{b}_{14} \\ \bar{c}_{11} & \bar{c}_{12} & \bar{c}_{13} & \bar{c}_{14} \end{bmatrix}$ and $\xi(t,u(t))$ consists of matched and unmatched uncertainties satisfying the condition $\left|\xi(t,u(t))\right| \le \xi(t,u(t))_{\max}$. The variables mentioned in $f(x)$ and $g(x)$ are described below:-

$a_1 = \beta_x\sin(2\phi)$, $a_2 = -\beta_y\sin(2\phi)$, $a_3 = 2\cos^2(\phi)(\beta_x - \beta_y)$,

$a_4 = 2F_{ex}\sin(\phi)\sin(\psi)$, $a_5 = 2F_{ex}\cos(\phi)\cos(\psi)$,

$b_1 = -\beta_x\sin(2\phi)$, $b_2 = \beta_y\sin(2\phi)$, $b_3 = 2\cos^2(\phi)(\beta_x - \beta_y)$,

$b_4 = -2F_{ex}\sin(\phi)\cos(\psi)$, $b_5 = 2F_{ex}\cos(\phi)\sin(\psi)$,

$\bar{a}_{11} = \bar{a}_{13} = \frac{-\alpha}{2M}(\sin(\phi) + \cos(\phi))$,

$\bar{a}_{12} = \bar{a}_{14} = \frac{-\alpha}{2M}(\sin(\phi) - \cos(\phi))$,

$\bar{b}_{11} = \bar{b}_{13} = \frac{-\alpha}{2M}(\sin(\phi) - \cos(\phi))$,

$\bar{b}_{12} = \bar{b}_{14} = \frac{\alpha}{2M}(\sin(\phi) + \cos(\phi))$, and

$\bar{c}_{11} = -\bar{c}_{12} = -\bar{c}_{13} = \bar{c}_{14} = \frac{\alpha}{2I_q}(a+b)$.

III. CONTROLLER DESIGN

The objective here, is to develop a control law in presence of external force and matched and unmatched uncertainties, such that the robot can track the desired trajectory. Moreover, it should be noted that the trajectory to be followed by the robot is available beforehand due to known arena. In such scenario, utilization of robust adaptive controller, is more appropriate due to its reliability and efficiency to handle uncertainties and disturbances. The localization approach may not be feasible in such cases due to high computational overhead, dependency on the sensors and confined workspace.

A. Sliding mode control law

Let $x_d(t) \in R = [x_{qd} \quad y_{qd} \quad \phi_d]^T$ is the desired trajectory, $e(t) = x_d(t) - x(t)$ is the trajectory error, and $\sigma(t) = [\sigma_1(t) \quad \sigma_2(t) \quad \sigma_3(t)]^T$ is the sliding surface. The important condition for first order sliding mode control is that $\sigma(t) = 0$ and $\sigma(t)\dot{\sigma}(t) < 0$. To reduce the computation load during real-time implementation, conventional sliding surface is selected [10]

$$\sigma(t) = \left(\lambda_c + \frac{d}{dt}\right)^{n-1} e(t) \tag{15}$$

where λ_c is a positive constant and $n = 2$ being order of system. Differentiating (15) yields

$$\dot{\sigma}(t) = \lambda_c\dot{e}(t) + \ddot{e}(t) \tag{16}$$

Using (14), (16) is written as

$$\dot{\sigma}(t) = \lambda_c(\dot{x}_d(t) - \dot{x}(t)) + (\ddot{x}_d(t) - \{f(x) + g(x).u(t) + \xi(t,u(t))\}) \tag{17}$$

According to ideal sliding surface condition trajectory error $e(t)$ converge to zero as $\sigma(t) = 0$. Hence, reaching phase control law is obtained as

$$u_r(t) = g(x)^{-1}(\lambda_c(\dot{x}_d - \dot{x}) + \ddot{x}_d - f(x) + (\xi(t,u(t)))) \tag{18}$$

The control law mentioned in (18) is unable to converge the error in real environment when the uncertainties are present. Hence, to make the system robust against these uncertainties, switching function is incorporated for the sliding phase and the sliding phase control is defined as

$$u_{sw}(t) = g(x)^{-1}(G.sign(\sigma(t))) \tag{19}$$

where G is the switching gain. Hence, total control input

$$u_t(t) = u_r(t) + u_{sw}(t)$$
$$g(x)^{-1}(\lambda_c(\dot{x}_d - \dot{x}) + \ddot{x}_d - f(x) + (\xi(t,u(t)) \quad (20)$$
$$+ g(x)^{-1}(G.sign(\sigma(t)))$$

Due to use of sign function, as the value of G increases, chattering increases considerably, therefore boundary layer technique [10] is implemented where sign function is replaced by saturation function to eliminate the chattering and (20) becomes

$$u_t(t) = u_r(t) + u_{sw}(t)$$
$$g(x)^{-1}(\lambda_c(\dot{x}_d - \dot{x}) + \ddot{x}_d - f(x) + (\xi(t,u(t)) \quad (21)$$
$$+ g(x)^{-1}(G.sat(\sigma(t)))$$

where $sat(\sigma_i) = \begin{cases} sign(\sigma_i), & |\sigma_i| > \delta > 0 \\ \dfrac{\sigma_i}{\delta}, & |\sigma_i| \le \delta \end{cases}$, and δ is a small positive constant. However, it should be noted that use of saturation function may increase the control input.

B. Adaptive control law

The control law in (21) removes the chattering of the system as saturation function is used. However, system may face critical control when the mobile robot has to take a sharp turn, do backward movement or dynamics of the robot and uncertainties are varying. To control a robot in such scenario, tuning the value of switching gain is a tedious job. Hence, in this work the controller is made adaptive by defining an adaptive law as

$$\dot{\hat{a}}_\rho = \begin{bmatrix} \dot{\hat{a}}_{p1} & 0 & 0 \\ 0 & \dot{\hat{a}}_{p2} & 0 \\ 0 & 0 & \dot{\hat{a}}_{p3} \end{bmatrix}$$
$$= \lambda \begin{bmatrix} \sigma_1(t)sat(\sigma_1(t)) & 0 & 0 \\ 0 & \sigma_2(t)sat(\sigma_2(t)) & 0 \\ 0 & 0 & \sigma_3(t)sat(\sigma_3(t)) \end{bmatrix} \quad (22)$$

where $\hat{a}_\rho$ estimates the value of switching gain G and λ is a small positive constant. Now the total control input u_T for an adaptive robust controller can be modified as

$$u_t(t) = u_r(t) + u_{sw}(t)$$
$$g(x)^{-1}(\lambda_c(\dot{x}_d - \dot{x}) + \ddot{x}_d - f(x) + (\xi(t,u(t)) \quad (23)$$
$$+ g(x)^{-1}(\hat{a}_p.sat(\sigma(t)))$$

The stability of the proposed adaptive robust controller is guaranteed only if it satisfies by Lyapunov Theory [10]. For this aspect, following procedure is adopted:

Theorem: The trajectory error for FMWMR converges asymptotically to zero if control input is designed as in (23), provided the control design parameters λ_c, δ and λ (small positive constants) are chosen appropriately.

Proof: Let $\tilde{a}_{\rho i}\ (i = 1,2,3) = \hat{a}_{\rho i} - \bar{a}_{\rho i}$ is the estimated error where $\bar{a}_{pi}$ is the nominal value of $\hat{a}_{pi}$. Lyapunov function is selected as

$$V = \frac{1}{2}\sigma(t)^T\sigma(t) + \sum_{i=1}^{3}\frac{1}{2\rho_i}\tilde{a}_{\rho i}^2 \quad (24)$$

First time derivative of Lyapunov function is obtained as

$$\dot{V} = \sigma(t)^T\dot{\sigma}(t) + \sum_{i=1}^{3}\frac{1}{\rho_i}\tilde{a}_{\rho i}\dot{\hat{a}}_{\rho i} \quad (25)$$

Since, $\dot{\sigma}(t) = -\hat{a}_p sat(\sigma(t)) - \xi(t,u(t))$

and $\tilde{a}_{\rho i}\ (i = 1,2,3) = \hat{a}_{\rho i} - \bar{a}_{\rho i}$, (25) yields

$$\dot{V} = \sigma(t)^T(-\bar{a}_p sat(\sigma(t)) - \xi(t,u(t)))$$
$$+ \sum_{i=1}^{3}\tilde{a}_{\rho i}\left(-\sigma(t)_i sat(\sigma(t)_i) + \frac{\dot{\hat{a}}_{\rho i}}{\rho_i}\right) \quad (26)$$

The second term $\sum_{i=1}^{3}\tilde{a}_{\rho i}\left(-\sigma(t)_i sat(\sigma(t)_i) + \frac{\dot{\hat{a}}_{\rho i}}{\rho_i}\right)$ in (26) tends to zero for $t \ge 0$. Moreover, $\sigma(t)sat(\sigma(t)) = |\sigma(t)|$ and $|\sigma(t)|\xi(t,u(t)) = -\sigma(t)|\xi(t,u(t))|$, (26) is finally obtained as

$$\dot{V} = -\sum_{i=1}^{3}\sigma_i(t)sat(\sigma_i(t))(\bar{a}_{\rho i} - |\xi(t,u(t))|) \quad (27)$$

$\sigma(t)sat(\sigma(t)) = |\sigma(t)| \ge 0$ always and $\bar{a}_{\rho i}$ which depends upon $\hat{a}_{\rho i}$, ensures that $\bar{a}_{\rho i} \ge |\xi(t,u(t))|$. Therefore proper selection of design parameters satisfies the Lyapunov criterion i.e $\dot{V} \le 0$.

IV. Simulation Results

To demonstrate the effectiveness of proposed controller, simulations are performed for two different trajectories using Matlab/Simulink 2015a. Parameter values of FMWMR are selected as: $M = 6$ kg, $R = 0.05$ m, $a = 0.11$ m, $b = 0.18$ m, $I_q = 0.0945$ m^2, $\alpha = 0.087$ N/V and $\beta = 11.4$ kg/s.

A. Trajectory I

To prove the performance of proposed controller, desired trajectory is selected as $x = \frac{0.3\cos(t)}{1+\sin^2(t)}$, $y = \frac{0.9\sin(t)\cos(t)}{1+\sin^2(t)}$, $\phi = 0$. The bounded uncertainties used in the simulation is taken as

$$\xi(t,u(t)) = \begin{cases} |0.5| \ \forall\ 20\ s < t \le 26\ s \\ 0.9\sin(t)\ \forall\ t \ge 50\ s \\ 0 \end{cases}$$

. Range of λ_c is selected such that error $e(t) \to 0$. Higher value of λ_c minimizes the error but increases the control input. Hence, optimal value of λ_c is calculated by pattern search optimization method and is obtained as 22.7. In order to keep the sliding surface proper selection of λ is necessary. Increasing the value of λ brings the sliding function to zero. Accordingly, the value calculated as per optimization technique is obtained as 4.7. δ is taken as 0.1.

Fig. 3 shows simulation results for the desired trajectory. As can be seen from Fig. 3(a), the proposed controller is

capable of tracking the desired trajectory in a more efficient way as compared to PID controller. Fig. 3(b) shows chattering free control input voltage at each wheel with $U_{C.E} = [664.49 \quad 651.54 \quad 664.49 \quad 651.54]^T$ Nm which is the control energy calculated using 2-norm method. The rise in control input voltage between 20 s to 26 s is because of uncertainties. The time history of estimated adaptive gain

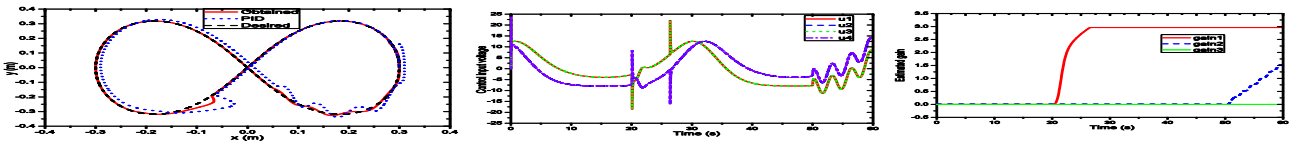

(a) (b) (c)

Figure 3: Simulation results for trajectory I showing trajectory, control input voltage and estimated gain.

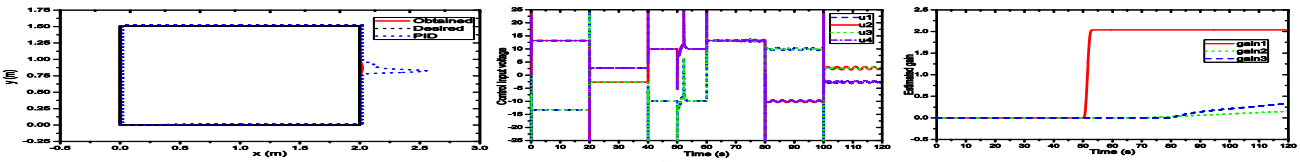

(a) (b) (c)

Figure 4: Simulation results for trajectory II showing trajectory, control input voltage and estimated gain.

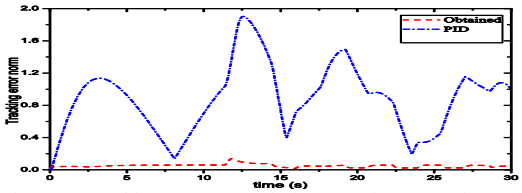

Figure 5: Tracking error norm during experiment (Trajectory I)

TABLE I. Tracking performance comparison (Trajectory I)

Controller	ISE (m)	IAE (m)	ITAE (m)
Proposed	$[6 \quad 3.64 \quad 2.1]^T e-2$	$[9.7 \quad 7.11 \quad 2]^T e-1$	$[0.28 \quad 0.33 \quad 0.13]^T$
PID	$[3.9 \quad 1.4 \quad 2.7]^T$	$[88 \quad 71 \quad 64]^T$	$[100 \quad 104.1 \quad 97.08]^T$

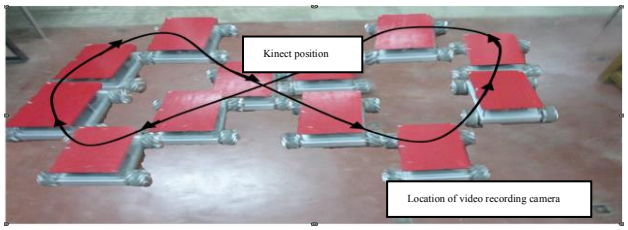

Figure 6: Overlay of several snapshots while performing trajectory I

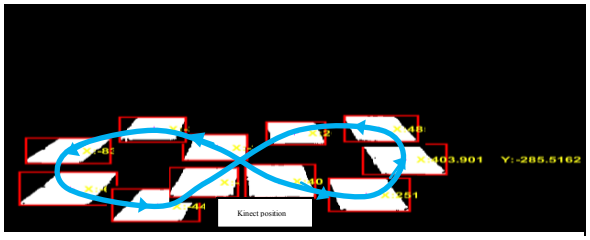

Figure 7: Image processing through Kinect for trajectory I

Figure 8: Overlay of several snapshots while performing trajectory II

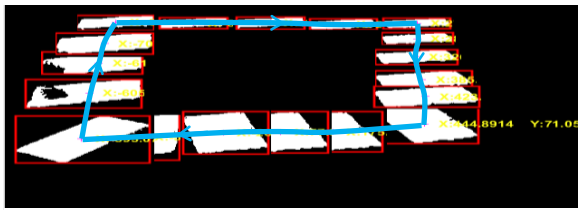

Figure 9: Image processing through Kinect for trajectory II

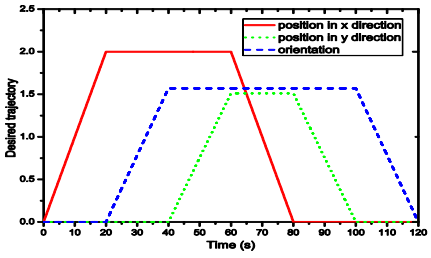

Figure 10: Desired position and orientation.

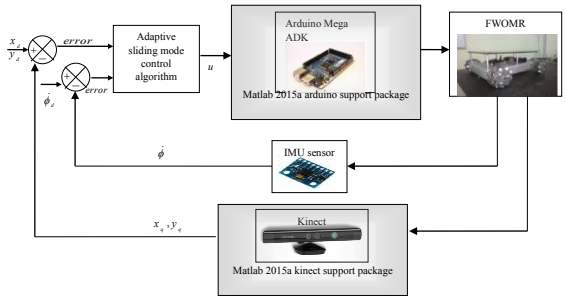

Figure 11: Block diagram for real time implementation.

$\hat{a}_\rho$ is shown in Fig. 3(c), which shows that the gain is state dependent. Hence, the gain value can be tuned automatically.

B. *Trajectory II*

To check the capability of the controller to track the angular trajectory, the desired x_{qd}, y_{qd}, and ϕ are selected as shown

in Fig. 10. For the simulations uncertainty is selected as

$$\xi(t,u(t)) = \begin{cases} |0.5| \forall\ 50\ s < t \le 53\ s \\ 0.1\sin(t) \forall\ t \ge 80\ s \\ 0 \end{cases}$$

Design parameters for proposed controller is based on criterion as discussed in section A. The values calculated from pattern search optimization method are 30.6, 7.8, 0.5 for λ_c, λ and δ respectively. The simulation results for the desired trajectory is presented in Fig. 4. It is evident from Fig. 4(a) that compared to PID controller the proposed controller is efficient enough to track the trajectory even when the angular displacement of FMWMR is non zero. Moreover, the control input voltage at each wheel is shown in Fig. 4(b) and has calculated control energy, $U_{C.E} = [1435 \quad 1435 \quad 1413 \quad 1413]^T$ Nm. The high value of control energy is associated with sharp turns of FMWMR and introduction of uncertainties at various intervals. Finally state dependent adaptive gain variation with respect to time can be seen in Fig. 4(c).

V. Experiments

For validation of simulation results, the control algorithm with dynamics has been implemented on FMWMR. Fig. 11 shows the block diagram for real time implementation of the proposed controller on the robot. The obtained control input voltage command is sent to the mobile robot using Arduino MEGA ADK. To send the signals to the Arduino board, PWM and digital output block, available in Matlab/Simulink Arduino support package has been utilized. The real time position data is provided by Kinect color based object tracking. As the orientation values can't be calculated with the knowledge position data, like in conventional mobile robots, Inertial Measuring Unit (IMU) has been mounted on the robot to acquire the same.

The experiments are performed on a horizontal plane surface with no obstacles. From (14), it is evident that including uncertainties will deviate the mobile robot. So, in real scenario, if there is a deviation of the mobile robot from the desired trajectory, which may be for example because of surface roughness, or slippage, the controller will make the system robust and adaptive against these changes. Moreover, to make the experiments more challenging, same uncertainties as in simulations were fed to the mobile robot through program which was not known to the controller. Fig. 6 and Fig. 8 shows the overlay of several snapshots while performing trajectory I and trajectory II respectively in real time. The upper surface of the robot has been colored red, so that the Kinect tracks the c.g of the bounded rectangular area as shown in Fig. 7 and Fig. 9 for trajectory I and II respectively. Fig. 5 shows the tracking error norm variation with time for trajectory I during real time implementation. It can been seen that in a real environment the proposed controller is able to track the desired path in presence of uncertainties with less tracking error norm ,compared to the conventional PID controller. In order to compare the tracking performance of the proposed controller and PID controller the values of integrated square error (ISE), integral absolute error (IAE), and integral time weighted error (ITAE) for trajectory I has been presented in Table I which proves the superiority of the adaptive robust controller over PID controller. Results obtained shows that while tracking the trajectory there is an error due to drift which is associated with high torque requirement during the turns. Another reasons for error in real time implementation can be related to delay in position and orientation data transfer and slippage of rollers mounted on the periphery of the wheels.

VI. Conclusion

In this paper, we have proposed a robust adaptive controller for a FMWMR in presence of external disturbance and uncertainties which allows the robot to track any complicated trajectory. First, equation of motion is derived. Then we have derived an adaptive sliding mode control law for the robot. Later, the asymptotic stability of the proposed control law is satisfied by Lyapunov stability theorem. The derived control law is implemented for two different types of trajectories which proved that the controller is able to track the desired trajectory with minimum error and less chattering of control input voltage. Further, for real time implementation of the present work experiments are performed using Kinect and IMU as position and orientation sensor respectively and it was found that despite of error due to drift while turning, slippage and delay in sensor data transfer, FMWMR is able to track the desired trajectory.

VII. References

[1] F. G. Pin and S. M. Killough, "New family of omnidirectional and holonomic wheeled platforms for mobile robots," *IEEE Trans. Robot. Autom.*, vol. 10, no. 4, pp. 480–489, 1994.

[2] a. S. Conceicao, a. P. Moreira, and P. J. Costa, "Practical approach of modeling and parameters estimation for omnidirectional mobile robots," *Mechatronics, IEEE/ASME Trans.*, vol. 14, no. 3, pp. 377–381, 2009.

[3] N. Tlale and M. de Villiers, "Kinematics and Dynamics Modelling of a Mecanum Wheeled Mobile Platform," *2008 15th Int. Conf. Mechatronics Mach. Vis. Pract.*, no. 4, pp. 657–662, 2008.

[4] J.-M. Yang and J.-H. Kim, "Sliding mode control for trajectory tracking of nonholonomic wheeled mobile robots," *Robot. Autom. IEEE Trans.*, vol. 15, no. 3, pp. 578–587, 1999.

[5] N. Adhikary and C. Mahanta, "Integral backstepping sliding mode control for underactuated systems: Swing-up and stabilization of the Cart-Pendulum System," *ISA Trans.*, vol. 52, no. 6, pp. 870–880, 2013.

[6] N. Chen, F. Song, G. Li, X. Sun, and C. Ai, "An adaptive sliding mode backstepping control for the mobile manipulator with nonholonomic constraints," *Commun Nonlinear Sci Numer Simulat .*,vol. 18, pp. 2885–2899, 2013.

[7] J. Huang, T. Van Hung, and M. Tseng, "Smooth Switching Robust Adaptive Control for Omnidirectional Mobile Robots," *IEEE Trans on Control Systems Technology*., pp. 1–8, 2015.

[8] Patrick F. Muir and CHrles P.Neuman, "Kinematic modeling for feedback control of an omnidirectional wheeled mobile robot," *Proceesings of International Conference on Robotics and Automation*, pp.1772-1778,1987

[9] T. D. Viet, P. T. Doan, N. Hung, H. K. Kim, and S. B. Kim, "Tracking control of a three-wheeled omnidirectional mobile manipulator system with disturbance and friction," *J. Mech. Sci. Technol.*, vol. 26, no. 7, pp. 2197–2211, Jul. 2012.

[10] Stoline. E, Weiping Li, "Applied Non Linear Control,"., Prentice Hal,1991.